Free Volume and Transport Properties in Highly Selective Polymer Membranes

C. Nagel,[†] K. Günther-Schade,[‡] D. Fritsch,[§] T. Strunskus,[⊥] and F. Faupel*[,‡]

Technische Fakultät der Christian-Albrechts-Universität zu Kiel, Lehrstuhl für Materialverbunde, Kaiserstrasse 2, D-24143 Kiel, Germany, and Institut für Chemie, GKSS Forschungszentrum GmbH, Max-Planck-Strasse, D-21502 Geesthacht, Germany

Received June 15, 2001; Revised Manuscript Received November 15, 2001

ABSTRACT: Varying systematically the structure of glassy poly(amide imide), poly(ester imide), and polyimide, we have studied the correlation between free volume and transport properties of highly selective polymer membranes. Free volume data were determined by means of positron annihilation lifetime spectroscopy (PALS) while transport properties originate from time-lag measurements of permanent gases. We find a good correlation between PALS average hole size and transport coefficients. The correlation is much better than with free volume data from group contribution methods. It is shown that the permeation properties are controlled not only by free volume fluctuations but also by energy barriers. A modified transport model taking into account the effect of the cohesive energy density on the energy barriers further improves the correlation significantly.

1. Introduction

Polymer membranes are of great technological interest. They play an important role in gas separation, especially for oxygen enrichment in combustion processes, in the medical sector, e.g., in the artificial lung, in nitrogen enrichment in petrochemical processing, and in food packing.[1]

The most important physical constants for gas separation are permeability P, which is the product of gas flux and membrane thickness divided by the pressure difference across the membrane and permselectivity $\alpha = P_A/P_B$, where A denotes the more permeable and B the less permeable gas. These properties are strongly dependent on the polymer structure. Normally a polymer with high permeability has low selectivity, but at a given permeability polymers differ in selectivity, too. In membrane applications, however, polymers with high permeability and high selectivity are needed. This has stimulated many investigations during the past decades.[2−10] Free volume has proven to have a strong influence in diffusion and permeation properties.[11−16]

The present paper is concerned with the correlation between free volume and transport properties. We have systematically varied the structure of glassy poly(amide imide), poly(ester imide), and polyimide membranes. These rigid polymers were chosen because of their high selectivity in conjunction with appreciable permeability which makes them attractive for membrane applications.[17] The highly flexible and permeable rubbery polymer poly(dimethylsiloxane) (PDMS) was included for comparison. Transport properties were determined by means of the time-lag method, which is a convenient technique to determine permeability P, diffusivity D, and solubility S simultaneously. The time lag is the intersection of the linear extrapolation of the gas pressure vs time relationship and the time axis.[6] Although the macroscopic transport coefficients are crucial for the characterization of the membranes, they do not give much information on the atomic scale. Therefore, positron annihilation lifetime spectroscopy was employed to get information about the effect of the structural modifications on free volume. The pick-off lifetime of the $^3S_1$ state of positronium (orthopositronium, termed o-Ps in the following) was used to measure free volume hole sizes in the membranes directly. Our investigation shows that the permeation properties are not only controlled by free volume fluctuations and suggest to include the cohesive energy density as an additional parameter.

2. Experimental Section

Synthesis of the polymer membranes and the determination of the macroscopic transport properties have been described in detail before.[18,19] The film thicknesses varied between 20 and 70 nm. They were measured with a deltascope MP10 by Helmut Fischer GmbH & Co. KG, Germany, with the "magnetic induction" principle. The average values were taken of at least 10 measurements. The structures of the repeating units are given in Figures 1−3.

The polymer samples were characterized by means of conventional X-ray diffraction (XRD). No indications of crystallinity could be found even after longer annealing experiments (several hours at $T > 300$ °C under 10^{-5} mbar vacuum). The glass transition temperatures were measured using dynamic mechanical thermal analysis (DMTA) at a frequency of 1.6 s^{-1} and a heating rate of 2 K min^{-1}. The α-peak temperature of tan δ was chosen as the glass transition temperature T_g. This T_g is somewhat higher (10−20 K) than the one determined by tangent construction on the modulus curve. The corresponding weight losses at T_g, determined by TGA, were <1% for poly(amide imide)s and ≅2% for polyimides. The results of the sample characterization are given in Table 1.

To ensure similar conditions in the time-lag and positron annihilation measurements, all samples used for positron annihilation were soaked in methanol and subsequently held

[†] Present address: Fraunhofer-Institut für Fertigungstechnik und Angewandte Materialforschung, Wiener Strasse 12, D-28359 Bremen, Germany.

[‡] Technische Fakultät der Christian-Albrechts-Universität zu Kiel, Kaiserstr. 2, D-24143 Kiel, Germany.

[§] Institut für Chemie, GKSS Forschungszentrum GmbH, Max-Planck-Strasse, D-21502 Geesthacht, Germany.

[⊥] Present address: Lehrstuhl für Physikalische Chemie I, Ruhr-Universität Bochum, Universitätsstr. 150, D-44780 Bochum, Germany.

* Corresponding author.

10.1021/ma011028d CCC: $22.00
Published on Web 02/07/2002

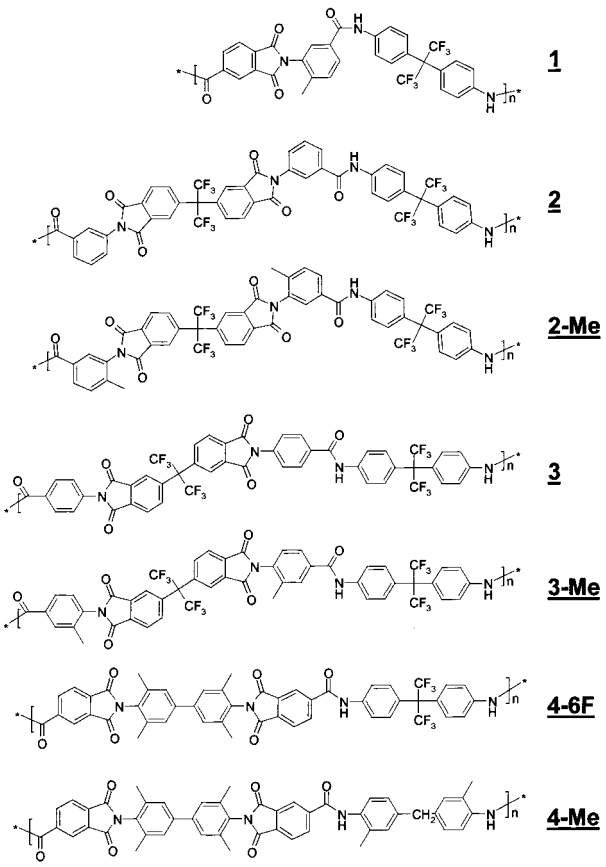

Figure 1. Chemical structures of the poly(amide imide)s, **1**, **2**, **2-Me**, **3**, **3-Me**, **4**−**6F**, and **4-Me**.

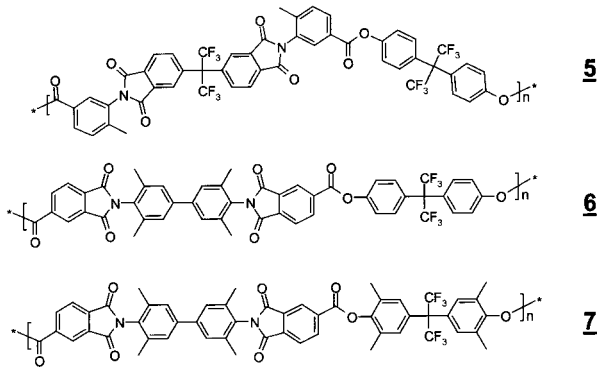

Figure 2. Chemical structures of the poly(ester imide)s **5**, **6**, and **7**.

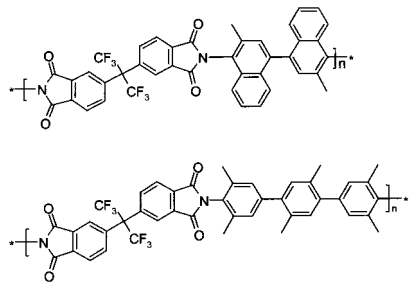

Figure 3. Chemical structures of the polyimides **8** and **9**.

in a vacuum (10^{-8} mbar) at 110 °C for 12 h to deaerate the films before the measurements. The samples were measured in standard source-sample sandwich geometry. To prevent annihilations in the surrounding media, the polymer films were stacked to a thickness of 0.5−0.7 mm. The measurements were done under vacuum conditions (10^{-6} mbar) at 30 °C to avoid influences of temperature, pressure, or humidity.

The positron lifetime spectra were measured using a fast−fast coincidence setup with Hamamatsu photomultipliers, Ortec electronic components, and Bicron BC420 scintillator material. The full width of half-maximum (fwhm) of the time resolution function was 230 ps. Measurements were performed with directly deposited sources as well as with encapsulated Kapton foils (30HN, Du Pont). The source activity were 30 ± 1 μCi. The counting rates were 300−400 s^{-1}. For each polymer, 10−15 spectra containing total counts of 3×10^6 and 6×10^6 were measured. The spectra were counted automatically without any time lag. The spectra were decomposed into three discrete lifetime components using the Patfit88 package.[20] The longest lifetime was attributed to o-Ps pick-off annihilation (τ_{o-Ps}). Since only the longest component was used, no source correction was needed. The positron lifetime in the Kapton source was 372 ps. The intensity of the source term was typically 4% for direct deposition and 12% for the Kapton foil source.

For calculation of the average hole size we used the so-called "standard model" where it is assumed that the Ps atom is confined to an infinitely deep spherical potential well:[21,22]

$$\tau_{o-Ps} = \lambda_0^{-1}\left(1 - \frac{R_h}{R_h + \delta R} + \frac{1}{2\pi}\sin\frac{2\pi R_h}{R_h + \delta R}\right)^{-1} \qquad (1)$$

In eq 1, the prefactor is the reciprocal spin-averaged Ps annihilation rate of 0.5 ns.[23] The quantity R_h is the radius of the hole, and the empirical parameter δR is the thickness of an electron layer describing the electron density of the surrounding molecules. The value of δR has been determined before to be 1.656 Å by fitting eq 1 to positron lifetime values measured in systems of known hole sizes.[24] This model seems to be generally accepted and has been used by most authors, unless there were extremely aspheric holes.[25,26] Equation 1 contains no free parameters, and the hole size can be directly calculated from the o-Ps lifetime. Because the o-Ps lifetime is expected to show a distribution in polymers, the discrete o-Ps lifetime obtained using the Patfit88 package actually represents a mean value. Thus, we use the term "average o-Ps lifetime" for τ_{o-Ps} and "average hole radius" R_h. The cavity volumes ("average hole sizes") were calculated from $V_h = 4\pi R_h^3/3$. Average o-Ps lifetimes and hole radii are given in Table 1.

3. Results and Discussion

From the overall chain structures of the polymers (see Figures 1−3) one can easily conclude that the investigated poly(amide imide)s, polyimides, and poly(ester imide)s are polymers with a stiff backbone. This is also reflected in the high T_g values (Table 1). To determine the influence of the molecular structure on free volume and gas permeation, the structural units were selectively varied. Afterward the average free volume hole sizes, the diffusion coefficients, and the permeation coefficients were measured. Additionally, average interchain spacings d were determined. Comparison of the measured quantities results in a deeper insight into inter- and intramolecular interactions.

3.1. Selection of Polymers. Seven poly(amide imide)s (PAIs),[18,19] three closely related poly(ester imde)s (PEIs),[27] and two polyimides (PIs) with very stiff building blocks[28] were chosen for comparison. The PAIs consist of two imide and two amide groups per repeating unit (except for PAI **1**, only one imide). The imide group may be linked meta (**1**, **2**, **2-Me**) or para (**3**, **3-Me**, **4**−**6F**, **4-Me**). Methyl groups present (**1**, **2-Me**, **3-Me**) hinder the rotation around the imide bond and contribute in addition to chain stiffness. The PEI **5** is similar in structure to PAI **2-Me** as PEI **6** is to PAI **4**−**6F**. PEI **7**

Table 1. Properties of the Polymers Shown in Figure 1[a]

polymer	T_g [°C]	T_β [°C]	d [Å]	τ_{o-Ps} [ps]	V_h [Å^3]	P_{O_2}	α_{O_2/N_2}	P_{CO_2}	α_{CO_2/CH_4}
1	355	214	5.50	2440 ± 10	140 ± 2	2.8	6.2	15	60
2	297		5.73	2620 ± 20	159 ± 2	2.3	6.5	11	45
2-Me	337	224	5.68	2980 ± 10	198 ± 2	8.3	5.2	44	45
3	351		5.75	2760 ± 20	174 ± 2	4.3	5.4	25	58
3-Me	344	175	5.68	3120 ± 20	214 ± 3	6.1	5.5	34	67
4−6F	386	146	5.85	2910 ± 10	190 ± 2	9.4	4.5	56	36
4-Me	329	146	5.60	2220 ± 60	118 ± 11	1.1	5.8	5.5	37
5	289	214	5.78	2960 ± 10	195 ± 1	8.8	5.0	47	43
6	335		5.85	2810 ± 10	179 ± 2	10.5	4.2	60	27
7	327		5.92	3150 ± 30	217 ± 7	18.9	4.4	110	31
8	403		6.27	4360 ± 10	364 ± 1	141	3.8	958	24
9	361	160	6.12	3870 ± 10	302 ± 1	55	4.1	234	19
PDMS	−123[b]					580	2.2	2800	3.4

[a] T_g and T_β are tan δ peak temperatures from DMTA at $\omega = 1.6$ s^{-1} and $\dot{T} = 2$ K min^{-1}. d-spacings were calculated from XRD measurements. Average o-Ps lifetimes and average hole sizes are given in columns 5 and 6. Permeation coefficients (in barrers) and permselectivities are presented in the last four columns. [b] DSC, taken from ref 38, p 761.

is identical to PEI **6** except for an additional four methyl groups ortho to the ester in the 6F unit. The imide group of PI **8** is linked to an ortho-methyl binaphthalene unit, whereas in PI **9** to a terphenylene derivative containing four methyl groups ortho to the imide.

3.2. Effects of Bulky Structural Units. Bulky structural units always hinder the chain packing. Therefore, free volume and permeability will increase. As an example, we compare the poly(amide imide)s **1** and **2-Me** (Figure 1). Because of the substituted aromatic rings, the imide units of both polymers are extremely stiff. The important difference is their size. Because of additional fluorine groups in the imide unit, **2-Me** is more bulky than **1** and the chain packing is more hindered. Therefore, the average hole volume is larger in **2-Me** (see Table 1). As a result, the permeability is 3 times larger, while there is only a minor decrease in permselectivity (Table 1). Similar effects can be obtained by replacing the diamines of the polyimides **8** and **9**.

3.3. Substitution of Side Groups. Methyl side groups increase the average hole size and the permeability.

Here introduction of four methyl groups ortho to the ester bonds in the poly(ester imide)s **6** and **7** increases the average hole size and the average d-spacing. Again, the increase in free volume can be explained by steric hindrance, which results in an increase of the average chain distance and a decrease of the chain packing density. (This effect is not compensated by the higher chain flexibility of the poly(ester imide)s.) As a result of the higher free volume, the permeability increases accompanied by maintaining or slightly increasing the selectivity.

Substitution of asymmetric methyl groups at the para-imide-phenylene of the poly(amide)s **3** and **3-Me** increases the average hole size. However, this is not reflected in the d-spacing. The permeabilities exhibit an increase by a factor of 1.3−1.5, in accordance with the higher average hole size.

Asymmetric methyl groups at the meta-imide-phenylene of the **2** and **2-Me** increase the average hole size. Permeabilities increase by a factor of 4. Apparently, the asymmetric CH_3 substitution is more effective for meta linkage than for para linkage.

3.4. Substitution in the Backbone. The influence of additional forces between chains is illustrated by comparing PAI to PEI (**4−6F**/**6** and **2-Me**/**5**). Replacing amide by ester groups slightly reduces the average hole size in **6** compared to **4−6F**, and in **2-Me**/**5** there is almost no change. It is interesting to note that there is no correlation between average hole size and permeabilities, which are ≈10% higher in the poly(ester imide)s compared to the poly(amide imide)s.

3.5. A Model for the Elementary Hopping Process. In the preceding sections the chain structures and their influences on inter- and intramolecular interactions were treated in a qualitative way. Now the data will be analyzed in terms of a quantitative transport model. In section 3.5.1 we apply the classical free volume model to our data and show some deficiencies of the model. In section 3.5.2 we will show how these deficiencies can be overcome by including an activation energy term.

Among all polymers investigated, the poly(ester imide)s exhibit the lowest selectivities but not the highest average hole sizes and permeabilities. This indicates that permselectivity may depend not only on chain stiffness but also on interchain interactions. Such interactions could be due to H-bridging and enhanced polarity caused by for example C═O and CF_3 groups. Both effects give rise to additional energy barriers which the gas molecules have to overcome in a diffusion jump. Finally, charge-transfer complexes may cause additional interactions in the present polymers; however, we do not have experimental proof. Contributions from H-bridges and polar groups are included in the cohesive energy density which can be estimated by using increment methods. In section 3.5.3 we interrelate activation energy of diffusion and cohesive energy density and demonstrate that the fit of the modified free volume model to experimental data can be improved. Finally, we present an atomistic interpretation of the model parameters and compare them to results from literature. This is done in section 3.5.4.

3.5.1. The Classical Free Volume Model. In Figure 4 the logarithms of diffusion coefficients of various gas molecules are plotted vs the reciprocal average hole sizes given in Table 1. This plot is suggested by the classical correlation between diffusion coefficient and free volume:

$$\log D = \log D_0 - \frac{B}{\ln 10 V_h} \qquad (2)$$

The specific free volume or the fractional free volume is frequently used[15,29−31] instead of the average hole size. The specific free volume is obtained by multiplying the average hole size with the number density N_0 of holes

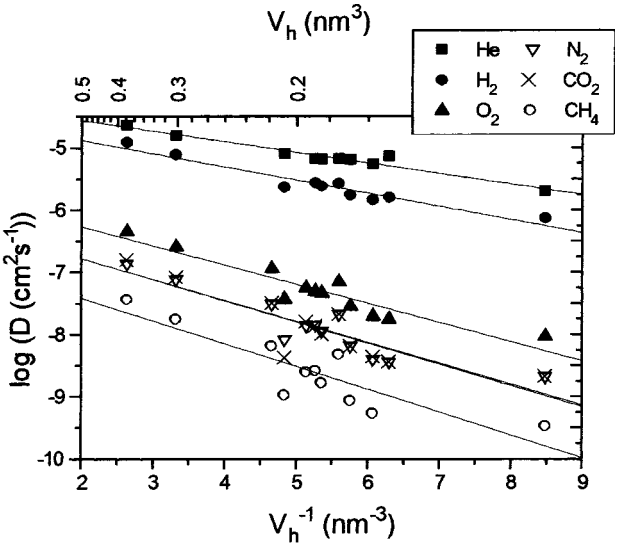

Figure 4. Plot of the logarithm of the diffusion coefficients of various gas molecules vs reciprocal average hole size from positron annihilation. Straight lines are linear regressions based on eq 2.

per gram of polymer, which may vary from polymer to polymer. N_0 can be absorbed into the parameter B. The physical interpretation of the parameters B and D_0 will be given below.

As predicted by free volume theories, a linear correlation is observed between log D and $1/V_h$.

Figure 4 shows that at a given hole size the different gases exhibit different diffusivities according to their size. This is the result of different availabilities of the free volume. For CH_4 the smallest fraction of unoccupied volume is available while for He the fraction is largest. In terms of the free volume approach, the size dependence is attributed to a critical volume fluctuation large enough for the diffusant to accomplish an elementary diffusion jump. The prefactor D_0 is smallest for CH_4, which will be interpreted below as being indicative of the largest activation energy (see eq 6).

Figure 4 reveals systematic deviations of the measured data from the regression lines which point to deficiencies of the simple free volume approach. The question as to whether there is a correlation between two random quantities X and Y can be answered by calculating the empirical correlation coefficient

$$R = \frac{\sum_{i=1}^{n}(x_i - \bar{x})(y_i - \bar{y})}{\sqrt{\sum_{i=1}^{n}(x_i - \bar{x})^2 \sum_{i=1}^{n}(y_i - \bar{y})^2}} \quad (3)$$

If $0 < R < 1$, X and Y are correlated. Anticorrelation results in $-1 < R < 0$, and $R = 0$ means no correlation at all.

For the present case we define the logarithmic deviation

$$\Delta_i^k = \log D_i^k - \log \bar{D}^k \quad (4)$$

of the measured diffusion coefficients from the regression line as a random quantity. The superscript denotes the gas species. Here the correlation coefficient is

$$R^{k,l} = \frac{\sum_{i=1}^{n}(\log D_i^k - \log \bar{D}^k)(\log D_i^l - \log \bar{D}^l)}{\sqrt{\sum_{i=1}^{n}(\log D_i^k - \log \bar{D}^k)^2 \sum_{i=1}^{n}(\log D_i^l - \log \bar{D}^l)^2}} \quad (5)$$

Values of the correlation coefficients are given in Table 2. For the gas species O_2, N_2, CO_2, and CH_4 R is nearly 1. So there is a strong correlation between the deviations from the regression lines. For H_2 and He the correlation is less pronounced. This might indicate that the diffusion mechanism for O_2, N_2, CO_2, and CH_4 is similar, while H_2 and He follow another diffusion mechanism. It can be expected that diffusion of He and H_2 is more of the interstitial type and that diffusion of these small diffusants can occur without major free volume fluctuations. The correlation coefficients involving H_2 and He are also affected by larger experimental errors due to the short time lags which give rise to larger scattering.

The diffusant-dependent systematic deviations from the regression lines can also be observed in the literature data[12,13] but have not yet been noticed except for a recent study[32] involving fractional free volume data according to Bondi.[33] The above correlation analysis clearly shows that the correlated deviations are caused by physical properties of the polymer matrices and cannot be described by the classical free volume theory.

3.5.2. Extension of the Classical Free Volume Theory. Further evidence of the view that diffusion of gas molecules in polymers is not only controlled by free volume can be obtained by comparing the present results with data reported in the literature,[13,29] which were measured by means of the same techniques but in strongly different polymer matrices. A corresponding plot is displayed in Figure 5. The striking observation is a strong essentially parallel shift between the regression lines for the two groups of polymers. This reveals strong differences in the diffusivity at a given free volume hole size depending on the polymer matrix. The parallel shift shows that these differences are not due to different exponents in eq 2 and can hence only be attributed to differences in the prefactor D_0 of diffusion.

The prefactor can be expressed in terms of a Boltzmann factor for thermal activation and a corresponding prefactor[34]

$$D_0 = D_0^0 \exp\left(-\frac{E}{kT}\right) \quad (6)$$

The activation energy E is generally attributed to the critical energy a penetrant molecule must obtain to overcome the attractive forces holding it to its neighbors. For simple gas molecules this energy is consequently neglected in view of the very weak interaction with the polymer matrix, and the Boltzmann term is absorbed into the prefactor D_0. This corresponds to the assumption of completely free-volume-controlled diffusion.[35,36] The parallel shifts of the regression lines in Figure 5 clearly reveal that this assumption is not justified even in the case of weakly interacting gas molecules.

The logarithmic deviation between two diffusion coefficients can be defined as

$$\Delta = \log D_1 - \log D_2 = -\frac{1}{kT \ln 10}(E_1 - E_2) \quad (7)$$

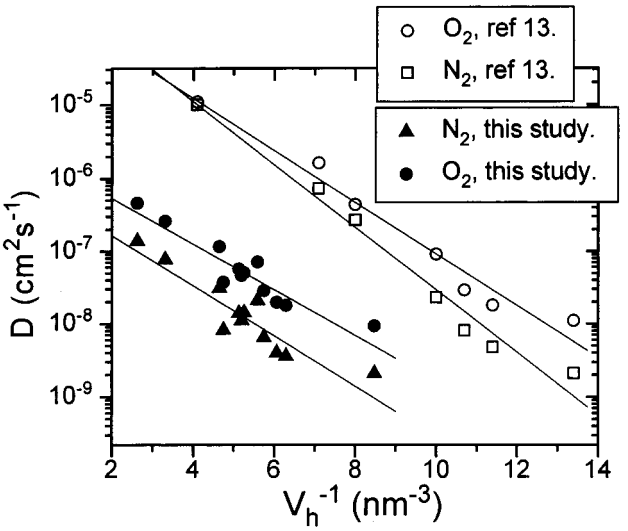

Figure 5. Plot of the logarithm of the diffusion coefficients of O_2 and N_2 vs reciprocal average hole size from positron annihilation. The straight lines result from linear regressions based on eq 2. Filled symbols result from the present experiments involving the polymers shown in Figures 1−3 while open symbols originate from refs 13 and 29.

Table 2. Correlation Coefficients Defined in Eq 5 for the Data Shown in Figure 4

R	H_2	He	N_2	O_2	CO_2	CH_4
H_2	1.00	0.36	0.89	0.90	0.90	0.92
He	0.36	1.00	0.08	0.12	0.11	0.24
N_2	0.89	0.08	1.00	1.00	0.99	1.00
O_2	0.90	0.12	1.00	1.00	0.99	0.99
CO_2	0.90	0.11	0.99	0.99	1.00	0.99
CH_4	0.92	0.24	1.00	0.99	0.99	1.00

For the diffusion coefficients in Figure 5 the difference in the activation energy between the data taken from ref 10 and the present one is $\Delta E \approx 50$ meV. This is of the order of 10% of measured activation energies.[7] This difference can be explained by differences in the polymer structures. The structure of the polymers studied by Kobayashi et al. is much simpler because there are no substituted phenyl rings in the backbone. PDMS, PMP, and PS have particularly flexible backbones. BPA-PC, PSF, and PES have short building blocks coupled by a flexible ether link. Thus, the chain flexibility of the polymers from ref 13 is much higher. Additionally, the intermolecular interaction of these polymers should be much smaller due to the absence of polar groups and groups forming hydrogen bonds. Finally, these polymers cannot form charge transfer complexes giving rise to additional attractive intermolecular interactions which is the case for the polymers in our study. The present considerations strongly suggest to attribute the activation energy in eq 6 to the energy required to separate the polymer chains in the saddle point of a hopping event. This energy should be determined by the cohesive energy density of the polymer.

3.5.3. Correlation of Activation Energies with Polymer Cohesive Energy Density. Table 3 gives the cohesive energy density e_{coh} calculated using the method of Fedors[37] and the solubility parameter δ calculated from the cohesive energy density. For better statistics we added polymers from refs 12 and 38. The average values are $\bar{e}_{coh} = 750 \pm 30$ J cm^{-3} for our polymers, 700 ± 20 J cm^{-3} for the polymers from ref 12, and 380 ± 40 J cm^{-3} for all other polymers. Figure 6 depicts the logarithmic deviation Δ, calculated by means of eq 7 with 1 as experimental data and 2 as linear fit data, against the e_{coh} values of Table 3. The good correlation lends strong support to the notion that the cohesive energy density of the polymer affects diffusion of small penetrants.

A simple model for the activation energy E was given by Meares.[39] This model relates the activation energy E to the energy E_h which is needed to open a cylindrical hole of the length l with the diameter d of the gas molecule in a medium with the cohesive energy density e_{coh}:

$$E_h = 0.25\pi l d^2 e_{coh} \tag{8}$$

Here not the absolute value of E_h but only its dependence on the diameters d of the diffusants is of importance.

To further test the role of the cohesive energy, the polymers involved in Figure 4 were organized in three groups—$\Delta > 0$, $\Delta < 0$, and $\Delta = 0$—according to the logarithmic deviation Δ from the regression line. For each group the average cohesive energy density was determined, and activation energy differences were approximated as

$$\Delta E \cong \Delta E_h = 0.25\pi l d^2 \Delta \bar{e}_{coh} \tag{9}$$

Using the rough estimate $l = 0.5$ nm and substituting eq 9 into eq 7, we then performed a correlation analysis between $\log D - \Delta$ and $1/V_h$ for each gas. The resulting improvement in correlation, shown in Table 4, is considerable.

An additional test was carried out including all the polymers involved in Table 3, which also includes the highly flexible polymers PDMS and PMP. Here, because of the good statistics, we did not average the data. Moreover, instead of eq 8 we used the more general relation

$$\Delta = a + b e_{coh} \tag{10}$$

suggested by Figure 6, with adjustable coefficients a and b. The results of the correlation analysis between $\log D - \Delta$ and $1/V_h$ are given in Table 5. The strong improvement is obvious. Remarkably, the correlation for the very flexible polymers including PDMS having the lowest cohesive energy density is also improved. This indicates that the intermolecular interactions play an important role for the activation energy of diffusion. The remaining scattering in the data is expected to be mainly due to experimental uncertainties.

3.5.4. Atomistic Interpretation of the Model Parameters. The parameters resulting from a fit to the $\log D$ vs $1/V_h$ data in Figure 4 by means of the classical free volume relation, given in eq 2, are shown in Table 6. The D_0 values are of the order of those from Arrhenius plots of $\log D$ against $1/T$.[7] Substituting eq 8 into eq 6 yields

$$\log D_0 = -\frac{0.25\pi l e_{coh}}{kT \ln 10} d^2 + \log D_0^0 \tag{11}$$

In this equation the only free parameters are D_0^0 and l. A plot of $\log D_0$ vs d^2 yields $l \approx 0.5$ nm. This corresponds to a characteristic length of the cylinder in the model of Meares of about twice the diameter of the penetrant molecule, which seems to be a reasonable value and justifies the assumption made above. The values for d

Table 3. Calculated Cohesive Energy Densities e_{coh} (J cm^{-3}) and Resulting Solubility Parameters δ (J$^{1/2}$ cm$^{-3/2}$) According to Ref 37; Polymers Given in Columns 4−6 Are from Ref 12 and Polymers in Columns 7−9 Are from Ref 38

polymer	e_{coh}	δ	polymer	e_{coh}	δ	polymer	e_{coh}	δ
1	747.0	27.3	pPD	764.7	27.7	BPA-PC	528.9	23.0
2	696.0	26.4	pDiMPD	717.3	26.8	TMBPA-PC	360.3	19.0
2-Me	838.5	29.0	pTeMPD	679.2	26.1	BPZ-PC	572.2	23.9
3	696.0	26.4	pTrMPD	697.3	26.4	PMP	269.1	16.4
3-Me	838.5	29.0	mMPD	739.7	27.2	PMMA	320.1	17.9
4-6F	770.1	27.8	pp′ODA	738.8	27.2	PTMSP	250.8	15.8
4-Me	872.5	29.5	BAHF	580.9	24.1	PEMA	318.3	17.8
5	736.5	27.1	APAP	665.5	25.8	PVAc	466.7	21.6
6	680.4	26.1	BATPHF	527.4	23.0	PDMS	228.2	15.1
7	642.9	25.4	4IU(75)	697.3	26.4	PS	466.0	21.6
8	824.6	28.7	4IU(50)	717.3	26.8			
9	638.5	25.3	4IU(25)	739.7	27.2			

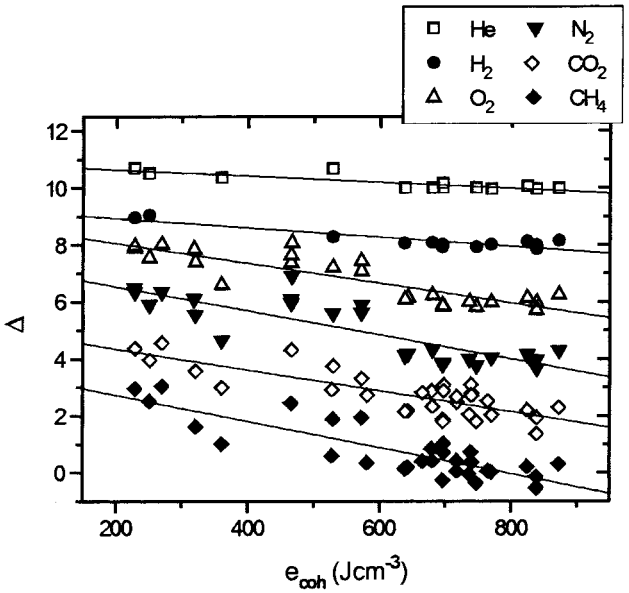

Figure 6. Logarithmic deviation Δ, calculated by means of eq 7 from the data in Figure 4, against cohesive energy density from Table 3. The data were shifted by constant values for sake of clarity.

Table 4. Squares of the Correlation Coefficients of log D − Δ and $1/V_h$ with (R_{corr}^2) and without (R^2) Taking into Account the Contribution of the Cohesive Energy Density According to Meares; Included Are Polymers Studied in This Work

penetrant	R^2	R_{corr}^2
He	0.91	0.95
H_2	0.94	0.98
O_2	0.88	0.95
N_2	0.85	0.92
CO_2	0.78	0.84
CH_4	0.77	0.85

Table 5. Squares of the Correlation Coefficients of log D − Δ and $1/V_h$ with (R_{corr}^2) and without (R^2) Taking into Account the Contribution of the Cohesive Energy Density According to Eq 10; Included Are All Polymers Given in Table 3

penetrant	R^2	R_{corr}^2
O_2	0.43	0.85
N_2	0.31	0.73
CO_2	0.39	0.68
CH_4	0.33	0.73

were taken from refs 40−42. Using these values and the value of l = 0.5 nm, one obtains activation energies E between 0.1 and 0.3 eV depending on the diameter of the gas molecule. These values are in the range of experimental values (E = 0.1−0.5 eV)

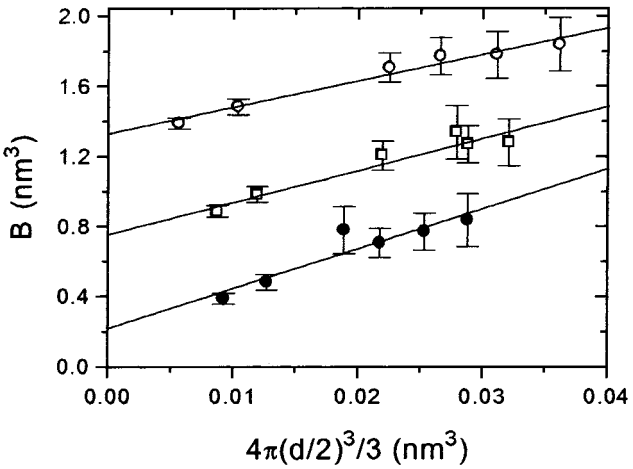

Figure 7. Free volume parameter B (eq 2) from Table 6 as a function of the volume of the gas molecules. The volume was calculated using the kinetic diameter from zeolite sieving experiments[40] (solid circles), Lennard-Jones collision diameters[38] (open squares), and diameters from viscosity measurements[42] (open circles).

Table 6. Parameters Resulting from a Fit of Eq 2 to the Data in Figure 4

penetrant	log D_0	B [nm^3]	R^2
He	−4.2 ± 0.1	0.39 ± 0.02	0.91
H_2	−4.5 ± 0.1	0.49 ± 0.04	0.94
O_2	−5.6 ± 0.2	0.71 ± 0.08	0.88
N_2	−6.1 ± 0.2	0.78 ± 0.10	0.85
CO_2	−6.1 ± 0.3	0.78 ± 0.12	0.78
CH_4	−6.7 ± 0.4	0.84 ± 0.14	0.77

reported for glassy polymers.[7] Details of the fits are given in ref 43.

The parameter B from Table 6 is plotted in Figure 7 as a function of the volume of the gas molecules using d values of different origin. One notes an essentially linear dependence on the gas volume as predicted by the free volume theory. According to the elaborated free volume model of Vrentas and Duda, B can be expressed as

$$B = \frac{\gamma \tilde{V}_1(0)}{N_0 M_j} \tag{12}$$

where γ is a free volume overlap factor of the order of 0.5 and $\tilde{V}_1(0)$ is the molecular gas volume at 0 K which can be estimated from the kinetic diameter or by other methods[36,44,45] yielding similar results. In eq 2 the hole free volume per gram of polymer of the Vrentas and Duda theory was taken as the product of the average hole volume from PALS and the number density of

holes: $\hat{V}_{FH}^{g} = V_h N_0$. The most uncertain parameter in eq 11 is the magnitude of the polymer jump unit M_j. In ref 36 it was shown that for many glassy polymers $M_j \approx 1.5 M_{mono}$, where M_{mono} is the molar mass of the monomer unit.

With the molar masses of the present polymers the number density of holes N_0 can be estimated from eq 11. We get $\overline{N_0} = N_0\rho = 2 \times 10^{19}$ cm^{-3} for the glassy polymers ($\rho = 1.3$ g cm^{-3}) and 1×10^{20} cm^{-3} for PDMS ($\rho = 1.02$ g cm^{-3}). This results in fractional free volumes of 0.008 for **8** and 0.03 for PDMS. N_0 values obtained from positron annihilation have to be taken with care since positronium is expected to reside preferentially in the larger holes.[46] This results in an underestimation of the number density of holes. Compared to the fractional free volumes determined by means of the increment method, the above values are very small. Although the deviations may partly be due to the crude approximations involved in the present estimation and in an underestimation of N_0, this seems to reflect that the free volume estimated by the Bondi method contains interstitial volume and hole volume, while gas transport is mainly controlled by the hole volume.

4. Conclusions

There is a good correlation between the average hole size taken from PALS and diffusivities of gas molecules. The correlation is considerably better than with free volume data according to the Bondi method. Apparently, average hole free volumes from PALS are well-suited to predict gas transport properties. On the other hand, the present investigation clearly reveals the influence of energy barriers on the diffusion behavior in the glassy state. These barriers are not due to interactions between gas molecules and the polymers but are correlated with the cohesive energy densities of the polymers. This was quantitatively taken into account in a modified transport model. Our experiments further suggest a strong influence of the energy barriers on the selectivity of gas separation membranes, which is also of considerable technological relevance. The selectivity can be increased by incorporation of strongly interacting groups in the polymer chain. These groups give rise to additional intermolecular forces which increase the cohesive energy and hence the energy barriers for diffusion jumps. The influence of energy barriers has also been suggested by molecular dynamics simulations.[47]

References and Notes

(1) Nakagawa, T. In *Polymeric Gas Separation Membranes*, 1st ed.; Paul, D. R., Yampol'skii, Y. P., Eds.; CRC: Boca Raton, FL, 1994; p 399.
(2) Frisch, H. L.; Stern, S. A. *Crit. Rev. Solid State Mater. Sci.* **1983**, *11*, 123−187.
(3) Paul, D. R.; Yampol'skii, Y. P. *Polymeric Gas Separation Membranes*; CRC: Boca Raton, FL, 1994.
(4) Stern, S. A.; Trohalaki, S. In *Barrier Polymers and Structures*; Koros, W. J., Ed.; ACS Symposium Series Vol. 423; American Chemical Society: Washington, DC, 1990.
(5) Vieth, W. R. *Diffusion in and through Polymers*; Hanser: Munich, 1991.
(6) Mulder, M. *Basic Principles of Membrane Technology*; Kluwer Academic Publisher: Dordrecht, 1996.
(7) Faupel, F.; Kroll, G. Diffusion in Glassy and Semicrystalline Polymers. In *Diffusion in Semiconductors and Non-Metallic Solids*; Landolt-Börnstein New Series Vol. III/33B; Martienssen, W., Beke, D. L., Eds.; Springer: Berlin, 1999; Chapter 9.
(8) Tanaka, K.; Kawai, T.; Kita, H.; Okamoto, K.; Ito, Y. *Macromolecules* **2000**, *33*, 5513−5517.
(9) Hirayama, Y.; Yoshinaga, T.; Kusuki, Y.; Ninomiya, K.; Sakakibara, T.; Tamari, T. *J. Membr. Sci.* **1996**, *111*, 183−192.
(10) Shantarovich, V. P.; Kevdina, I. B.; Yampolskii, Yu. P:, Alentiev, A. Yu. *Macromolecules* **2000**, *33*, 7453−7466.
(11) Pixton, M. R.; Paul, D. R. In *Polymeric Gas Separation Membranes*, 1st ed.; Paul, D. R., Yampol'skii, Y. P., Eds.; CRC: Boca Raton, FL, 1994; p 83.
(12) Tanaka, K.; Katsube, M.; Okamoto, K.; Kita, H.; Sueoka, O.; Ito, Y. *Bull. Chem. Soc. Jpn.* **1992**, *65*, 1891−1897.
(13) Kobayashi, Y.; Haraya, K.; Hattori, S. *Polymer* **1994**, *35*, 925−928.
(14) Jean, Y. C.; Yuan, J. P.; Liu, J.; Deng, Q.; Yang, H. *J. Polym. Sci., Part B: Polym. Phys.* **1995**, *33*, 2365−2371.
(15) Park, J. Y.; Paul, D. R. *J. Membr. Sci.* **1997**, *125*, 23−39.
(16) Trohalaki, S.; DeBolt, L. C.; Mark, J. E.; Frisch, H. L. *Macromolecules* **1990**, *23*, 813−816.
(17) Freeman, B. D. *Macromolecules* **1999**, *32*, 375−380.
(18) Fritsch, D.; Peinemann, K. V. *J. Membr. Sci.* **1995**, *99*, 29−38.
(19) Fritsch, D.; Avella, N. *Macromol. Chem. Phys.* **1996**, *197*, 701−714.
(20) Kirkegaard, P.; Pedersen, N. J.; Eldrup, M. *Risø-M-2740*; Risø National Laboratory: Denmark, 1989.
(21) Tao, S. J. *J. Chem. Phys.* **1972**, *56*, 5499−5510.
(22) Eldrup, M.; Lightbody, D.; Sherwood, J. N. *Chem. Phys.* **1981**, *63*, 51−58.
(23) Ferrante, G. *Phys. Rev.* **1968**, *170*, 76−80.
(24) Jean, Y. C. *Microchem. J.* **1990**, *42*, 72−102.
(25) Ciesielski, K.; Dawidowicz, A. L.; Goworek, T.; Jasinska, B.; Wawryszczuk, J. *Chem. Phys. Lett.* **1998**, *289*, 41−45.
(26) Jean, Y. C.; Shi, H. *J. Non-Cryst. Solids* **1994**, *172*, 806−814.
(27) Fritsch, D. In *Polymer Membranes for Gas and Vapor Separation*; Freeman, B. D., Pinnau, I., Eds.; ACS Symposium Series Vol. 733; American Chemical Society: Washington, DC, 1999.
(28) Al-Masri, M.; Kricheldorf, H. R.; Fritsch, D. *Macromolecules* **1999**, *32*, 7853−7858.
(29) Haraya, K.; Hwang, S. T. *J. Membr. Sci.* **1992**, *71*, 13−27.
(30) Tanaka, K.; Okano, M.; Toshino, H.; Kita, K.; Okamoto, K. *J. Polym. Sci., Part B: Polym. Phys.* **1992**, *30*, 907−914.
(31) Tanaka, K.; Kita, H.; Okano, M.; Okamoto, K. *Polymer* **1992**, *33*, 585−592.
(32) Thran, A.; Faupel, F.; Kroll, G. *J. Polym. Sci., Part B: Polym. Phys.* **1999**, *37*, 3344−3358.
(33) Bondi, A. In *Physical Properties of Molecular Crystals, Liquids and Glasses*; Bondi, A., Ed.; 1968; p 25.
(34) Vrentas, J. S.; Duda, J. L. *J. Polym. Sci., Part B: Polym. Phys.* **1977**, *15*, 403−416.
(35) Vrentas, J. S.; Vrentas, C. M. *J. Polym. Sci., Part B: Polym. Phys.* **1993**, *31*, 69−76.
(36) Zielinski, J. M.; Duda, J. L. *AlChE J.* **1992**, *38*, 405.
(37) Fedors, R. F. *Polym. Eng. Sci.* **1974**, *14*, 147−154.
(38) van Krevelen, D. W. In *Properties of Polymers*, 3rd ed.; van Krevelen, D. W., Ed.; Elsevier: Amsterdam, 1990; p 189.
(39) Meares, P. *J. Am. Chem. Soc.* **1954**, *76*, 3415−3422.
(40) Breck, D. W. In *Zeolite Molecular Sieves*; John Wiley & Sons: New York, 1974; p 636.
(41) van Krevelen, D. W. In *Properties of Polymers*, 3rd ed.; van Krevelen, D. W., Ed.; Elsevier: Amsterdam, 1990; p 535.
(42) Pace, R. J.; Datyner, A. *J. Polym. Sci., Polym. Phys. Ed.* **1979**, *17*, 437−451.
(43) Nagel, C. Ph.D. Thesis, University of Kiel, Germany, 1999.
(44) Sugden, S. *J. Chem. Soc.* **1927**, 1780−1785.
(45) Biltz, W. *Raumchemie der festen Stoffe*; Voss: Leipzig, 1934.
(46) Nagel, C.; Schmidtke, E.; Günther-Schade, K.; Hofmann, D.; Fritsch, D.; Strunskus, T.; Faupel, F. *Macromolecules* **2000**, *33*, 2242−2248.
(47) Sok, R. M.; Berendsen, H. J. C.; van Gunsteren, W. F. *J. Chem. Phys.* **1992**, *96*, 4699−4704.

MA011028D